

Electrophosphorescent devices with solution processible emitter and hole transport layer stack

Jae Kyun Park^a, Gyoung Seok Hwang^a, Byung Doo Chin^{a,*}, Nam Su Kang^b, Tae-Woo Lee^c

^aDepartment of Polymer Science and Engineering, Dankook University, Yongin, 448-701, South Korea

^bDisplay and Nanosystem Laboratory, College of Engineering, Korea University, Seoul 136-713, South Korea

^cDepartment of Materials Science and Engineering, Pohang University of Science and Technology, Pohang, 790-784, South Korea

ARTICLE INFO

Article history:

Received 31 October 2010

Accepted 20 April 2011

Available online 28 April 2011

Keywords:

Electrophosphorescence

Soluble

Interface

Ionomer

ABSTRACT

The light emitting behavior of the electrophosphorescent devices with solution-processible hole transport layer and light emitting layer was characterized. We have introduced the hole-transporting stacked layer composed of poly(3,4-ethylenedioxy thiophene): poly(4-styrenesulfonate) [PEDOT:PSS] and thin perfluorinated ionomer, aiming for the improvement of charge injection and transport with corresponding high efficiency behavior. In order to provide a suitable work function, composition and thickness of the ultra-thin perfluorinated ionomer was optimized for being an interfacial layer condition; 34 cd/A of green phosphorescent device was obtained while the control device without ionomer shows the luminous efficiency of 29 cd/A. Both for devices with vacuum-deposited and solution-processed electrophosphorescent emitters, change of the device efficiencies were analyzed in terms of the work function, surface chemical composition, and charge conduction behavior.

© 2011 Elsevier B.V. All rights reserved.

1. Introduction

Organic light emitting devices (OLEDs) with phosphorescent emitters have attracted considerable attention for a development of large area device with improved efficiency. While the devices with vacuum-deposited phosphorescent emitters already achieved significant improvement of efficiency and lifetime suitable for commercial application (at least red and green emitters), development of new materials as well as tailoring the device structure for solution-processed phosphorescent emitters are still under research [1–3]. Efforts to develop solution processible or printable phosphorescent emitters are driven by the advantages of these materials for the fabrication of large area OLEDs, which require emitters with higher efficiencies than those of normal fluorescent polymeric materials. Engineering of interfacial layers such as charge injection/transport materials are also important technique for further improvement of high efficiency phosphorescent light emitting devices with soluble and printable emitters.

Since the contact of PEDOT:PSS (conventional hole injection layer for a solution-processible device) with light emitting layer may be a main source of unstable interface at phosphorescent devices, modification of the PEDOT:PSS surface with layer-by-layer

deposition method have been reported. A fabrication of molecularly engineered structures with stepped and graded electronic profiles, which presents a better control of hole injection and a blocking of electron leakage, were good examples [4–6]. However, in most instances, the polymer phosphorescence can be quenched at the interface on top of the low-triplet-energy-interfacial layers (such as polyfluorene-based interfacial layers). Intermixing of the interfacial layer with light emitting layer at the over-coating process also causes the quenching. Recently, by utilizing the hole transport and light emitting layer with cross-linkable small molecular elements, multilayer-structured soluble phosphorescent OLED with controllable interface and higher efficiency was reported [7].

In this study, we have introduced an interfacial layer material with easily controllable work function, a perfluorosulfonate ionomer (PFI), for the improvement of device performance with green phosphorescent emitters. When the PFI is mixed with PEDOT:PSS in different ratios and forming a self-organized graded conformation, the energy level of the mixture layer on top of ITO could be precisely controlled [8]. In case of the layered over-coating of PEDOT:PSS and PFI, forced spatial distribution of PSS contents with different fluorinated backbone concentration can be provided. The surface chemical properties and work functions were investigated by X-ray photoelectron spectroscopy (XPS), time-of-flight secondary ion mass spectroscopy (TOF-SIMS), and ultraviolet photoelectron spectroscopy (UPS), providing an explanation on the electrical and luminous

* Corresponding author. Tel.: +82 31 8005 3587; fax: +82 31 8021 7218.
E-mail address: bdchin@dankook.ac.kr (B.D. Chin).

Table 1

The surface chemical properties and work function levels for PEDOT:PSS and selected PEDOT:PSS/PFI interfacial layers.

Sample code	1st layer (PEDOT:PSS Baytron 4083)	2nd layer (concentration of PFI solution for over-coating)	Corrected intensity for CF_3	Intensity of ^{115}In	Intensity of ^{120}Sn	Ionization Potential (by Riken KeiKi AC2)
I-1	35 nm	×	57.98	433.93	21.09	4.94
I-4	35 nm	PFI:methanol 1:10 (v/v)	6510.76	5.56	1.71	5.34
I-5	35 nm	PFI:methanol 1:5 (v/v)	8797.34	2.48	0.54	5.47
I-6	35 nm	PFI:methanol 1:3 (v/v)	9162.705	3.48	1.30	5.64

Table 2Configuration of the hole injecting/transporting layer stack of PEDOT:PSS/PFI for green electrophosphorescent devices (vacuum-deposited emitter), showing the turn-on voltage, efficiency, and CIE 1931 color coordinates. Device structure: ITO/PEDOT:PSS/PFI/NPB (20 nm)/CBP:Ir(ppy)₃ (30 nm, 5%)/BALq (5 nm)/Alq₃ (25 nm)/LiF (1 nm)/aluminum (200 nm). Data for I-6 is not included, due to the significant increase of driving voltage (>15V@1000m²).

sample code	1st layer (PEDOT:PSS Baytron 4083)	2nd layer (concentration of PFI solution for over-coating)	Voltage at 10,000 cd/m ²	cd/A efficiency at 1000 cd/m ²	lm/W efficiency at 1000 cd/m ²	CIE 1931 (x,y)
I-1	30 nm	×	9.3	29.2	14.1	(0.31, 0.61)
I-2	30 nm	PFI:methanol 1:20 (v/v)	9.0	29.6	14.3	(0.31, 0.61)
I-3	30 nm	PFI:methanol 1:15 (v/v)	8.7	32.5	15.7	(0.31, 0.61)
I-4	30 nm	PFI:methanol 1:10 (v/v)	9.2	33.6	16.2	(0.31, 0.61)
I-5	30 nm	PFI:methanol 1:5 (v/v)	>10	23.4	7.7	(0.31, 0.62)
I-6	30 nm	PFI:methanol 1:3 (v/v)	>15	–	–	–

properties of devices with PEDOT:PSS/PFI/phosphorescent emitter interfaces.

2. Experimental details

The patterned ITO (indium tin oxide) substrates with a sheet resistance of 15 Ω /sq were cleaned by ultra-sonication in deionized water and isopropanol. They were rinsed again in a chamber filled by hot isopropanol vapor. The cleaned substrates were subjected to UV–O₃ treatment for 15 min. Onto this cleaned substrate, PEDOT:PSS (Baytron P TP A14083, H.C. Starck) was spun-coated. A perfluorinated resin solution (Nafion[®] ionomer), 5 wt.% in mixture of lower aliphatic alcohols and water (Aldrich), was used as received. This PFI in a mixture of water and alcohol (4.5:5.5, v/v) was diluted with methanol with 1:20, 1:15, 1:10, and 1:5, and then spun-coated on top of the thermally annealed (180 °C) PEDOT:PSS film followed by successive annealing (80 °C) in a nitrogen atmosphere. Tables 1 and 2 shows the concentration of PFI solution which was used for over-coating on PEDOT:PSS surface and corresponding device codes. A phosphorescent light emitting layer (30 nm; 4,4'-N,N'-dicarbazole-biphenyl [CBP] doped with 5% fac-Tris(2-phenylpyridine) iridium(III) [Ir(ppy)₃]) was deposited by thermal evaporation at a vacuum level of 2×10^{-7} Torr. In case of device fabrication with solution-processed emitter, 40 nm-thick layer composed of CBP, poly(9-vinyl carbazole) (PVK), and Ir(ppy)₃ (with weight ratio of 47.5:47.5:5) was spun-coated from toluene solution. 5 nm-thick-aluminum (III) bis(2-methyl-8-quinolino)4-phenyl phenolate (BALq) and tris(8-hydroxyquinoline)-aluminum (Alq₃; 250 nm) were used as hole blocker and electron transporting layer, respectively. Then, a thin layer of lithium fluoride and an aluminum cathode (250 nm) were thermally evaporated to complete the device. The highest occupied molecular orbital (HOMO) of the PEDOT:PSS with various thickness of PFI and other organic materials was estimated from the ionization potential by ultraviolet photoelectron spectroscopy in air (surface analyzer, model AC2, Riken Keiki, Co., Ltd., Japan). Lowest unoccupied molecular orbital (LUMO) levels were determined from ionization potential and energy gap values taken from the lower energy threshold of the absorption spectra. Fig. 1 shows the device structure and energy diagram of each components, with chemical structures of the materials we used to formulate the stack of hole injection/transport layer and light emitters. XPS

spectra were measured using a PHI Q2000 system with-monochromated aluminum K α source. The binding energies were calibrated to the C 1s peak at 284.8 eV. The luminance-current-voltage (L–I–V) and spectral characteristics of the devices were measured with a current/voltage source/measurement unit (Keithley 238) and a Minolta CS-1000.

3. Results and discussion

We have set the concentration of PFI solutions for the formation of interfacial layer on top of PEDOT:PSS, as seen in Tables 1 and 2 with specified sample codes for each condition. The S 2p core-level X-ray photoelectron spectra of a PEDOT:PSS and samples with PFI interfacial layer film on ITO are shown in Fig. 2a. The peaks at around 169 eV and 164.5 eV, that can be assigned to the PSS-/PSSH and sulfur atoms of PEDOT, start to disappear as the PFI interfacial layer covers the surface of PEDOT:PSS. In the C 1s spectra, local bonding configuration of between C and F was seen (Fig. 2b, at 292 eV for -CxFy of PFI), where the C–C/C–H peak of sample S1 (PEDOT:PSS) is decreasing with the formation of PFI interfacial layer. The

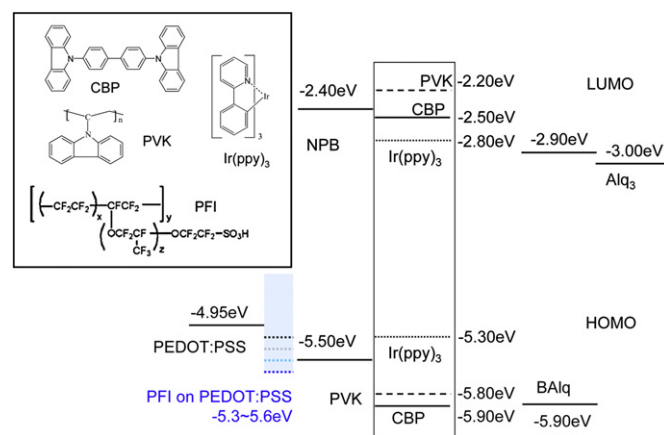


Fig. 1. Materials and schematic diagram of device structure and HOMO/LUMO energy levels for the components of hole injecting materials (layers of PEDOT:PSS/PFI), light emitting layers (vacuum-deposited - CBP:Ir(ppy)₃; solution coated - CBP:PVK:Ir(ppy)₃), blocking layer, and electron transport layer.

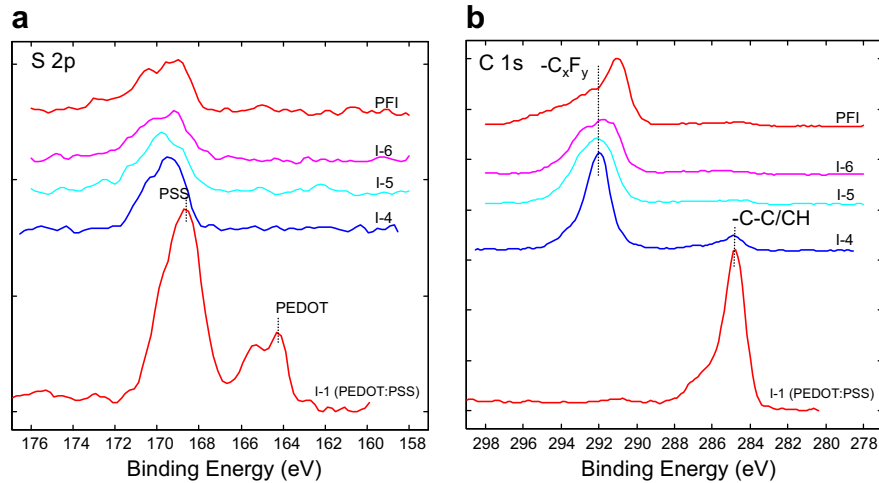


Fig. 2. XPS core-level spectra of S 2p (a) and C 1s (b) for the PEDOT:PSS/PFI surfaces with the variation of PFI thickness.

broadening of $-C_xF_y$ peak with increasing of PFI concentration might be explained by surface charging effect. Therefore, unlike the self-organizing PEDOT:PSS-PFI mixture, the surface properties of the PEDOT:PSS/PFI was dominated by the PFI, where the thickness can be precisely controlled. The increase of the intensity of CF_3 fragment (characteristics of PFI) was clear, which was shown in the corrected intensity data of CF_3 in Table 1 (from TOF-SIMS). Furthermore, the fluorinated surfaces induce effective reduction of In and Sn diffusion, showing the lowest intensities of ^{115}In and ^{120}Sn for the condition of I-5. Further increase of In and Sn residual intensity can be attributed to the dissolving of PEDOT:PSS at the over-coating of more concentrated PFI solution. The value of the ionization potential measured by Riken Keiki AC2 shows that increasing of PFI concentration yields lower HOMO level of PEDOT:PSS/PFI double layers.

Fig. 3 shows the relationship between current density vs. applied voltage and brightness vs. voltage characteristics of devices with various PEDOT:PSS/PFI layer thickness. The light emitting layer was 30 nm-thick vacuum-deposited CBP:Ir(ppy)₃ layer. The current density and brightness of the devices incorporating very thin interfacial layers of PFI from dilute concentration (I-2, and I-3) are higher through the whole range of bias voltage compared to control device. However, as the thickness of PFI increases (I-4 and I-5, approximately exceeding the thickness of

PEDOT:PSS; >50 nm), the current injection is rather hindered. Therefore, brightness is significantly reduced in case of I-5. In Fig. 4, luminous and power efficiency (cd/A and lm/W) of various devices are shown as a function of brightness. Again, devices with thin interfacial layer condition (I-2 and I-3) showed higher efficiency value compared to the control device. The maximum efficiency at 1000 cd/m² was 34 cd/A (16 lm/W) at device of I-4, while the lowest driving voltage was seen in device with I-3. The efficiency of control device was 29 cd/A (14 lm/W). Therefore, improved hole injection and transport by the insertion of thin PFI can be responsible for the achievement of high efficiency and low driving voltage behavior for electrophosphorescent devices. AC-2 measurement for PEDOT:PSS/PFI surface indicated that even infinitesimal increase of PFI thickness (I-3 and I-4) resulted in the shift of work function, providing 5.3–5.4 eV (optimum for facilitated hole transport than pristine PEDOT:PSS). Thus, tuning of energy level with thin PFI can support the efficient hole transport and improved efficiency. PFI itself, as a proton conductor, is not a good hole-transporting material, especially at thicker condition on PEDOT:PSS (as seen from the very high driving voltage of devices with I-6 PEDOT:PSS/PFI layer, which is not inserted in Table 2). The double layer coating of thin PFI on top of PEDOT:PSS,

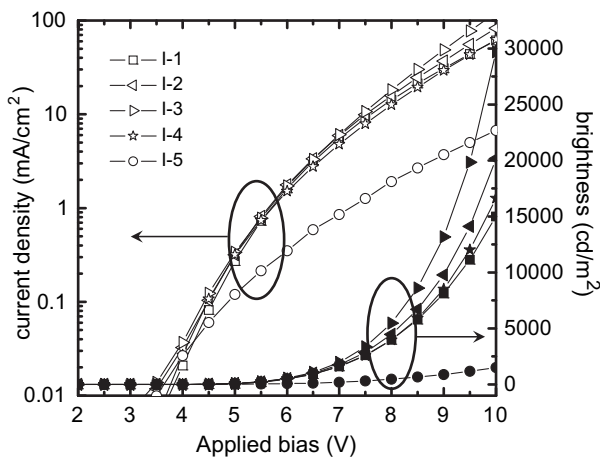


Fig. 3. Current density/brightness vs. bias voltage for the phosphorescent devices (vacuum-deposited emitter) with different PEDOT:PSS/PFI stacks of hole injecting/transporting layers.

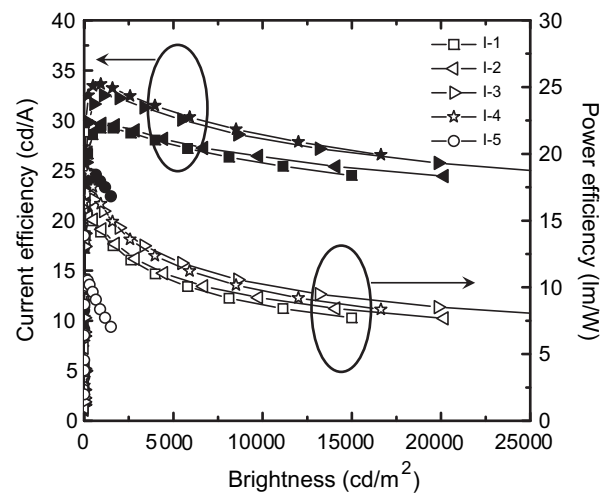


Fig. 4. Efficiency (cd/A and lm/W) vs. brightness characteristics for phosphorescent devices (vacuum-deposited emitter) with different PEDOT:PSS/PFI stacks of hole injecting/transporting layers.

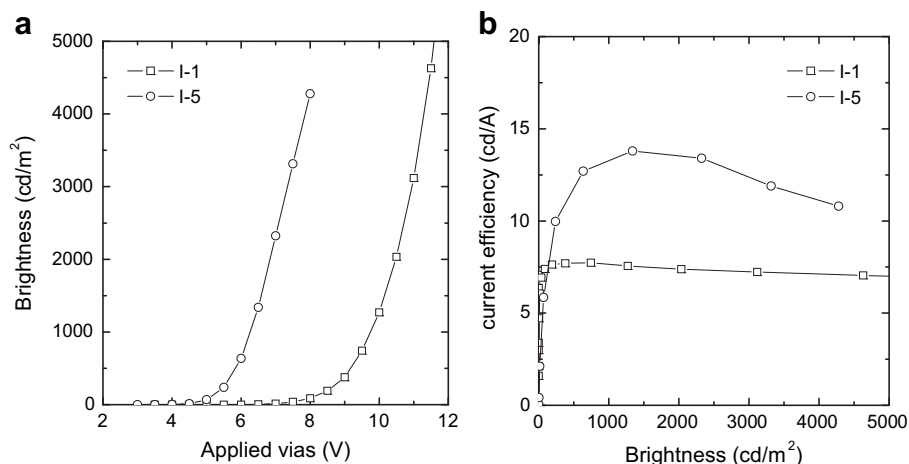


Fig. 5. The brightness vs. bias voltage (a) and current efficiency vs. brightness (b) for phosphorescent devices with solution-processed emitter (40 nm-thick-CBP:PVK:Ir(ppy)₃ blended film). Representative data for I-1 for bare PEDOT:PSS and I-5 for PEDOT:PSS/PFI hole injecting/transporting stack.

however, would be beneficial for the adjustment of work function as well as blocking of In/Sn diffusion for stable device operation. Completely covered thin PFI film on top of PEDOT:PSS (as seen in XPS spectra of Fig. 2b) shows the maximum efficiency at optimized condition (I-4), and then yields decreased efficiency as the thickness of PFI increases.

The improved efficiency of the interfacial layer-aided soluble phosphorescent devices can be explained by the assisted hole injection, while the quenching of the triplet exciton is a significant factor. In spite of the decrease of photoluminescent quantum yield (PLQY) induced by the triplet energy mismatch, use of the polyfluorene-based interfacial layers was a practical way to improve the charge injection from PEDOT:PSS to the emitting layer, which resulted in the enhanced brightness and current level for soluble phosphorescent devices [9,10]. The polyfluorene-based interfacial layers, however, was not effective for high efficiency behavior due to the interfacial triplet quenching [11]. Fig. 5 illustrates the current efficiency vs. brightness and brightness vs. bias voltage for solution-processed green phosphorescent devices with and without PFI interfacial layer. Compared to the control device with PEDOT:PSS/emitter contact, PEDOT:PSS/PFI/CBP:PVK:Ir(ppy)₃ emitter yields higher efficiency and brightness, which can be explained by the facilitated hole injection to the CBP:PVK:Ir(ppy)₃ emitting layer without quenching. The optimum thickness of PEDOT:PSS/PFI (I-5) changed to different condition compared to the set of data for vacuum-deposited emitting layers [NPB/CBP:Ir(ppy)₃], where I-4 shows the highest efficiency behavior. This can be explained by the dissolution of the PEDOT:PSS/PFI surface by the over-coating CBP:PVK:Ir(ppy)₃ light emitting layer on top of PFI surface. The maximum efficiency with soluble emitter device was about 13.5 cd/A at 1000 cd/m² while the control device was 7.8 cd/A. Further improvement of device efficiency as well as stability for soluble electrophosphorescent devices with PFI-interfacial layer might be achieved by use of shorter chain ionomer and precise engineering of work function with facilitated charge conduction at interface.

4. Conclusion

Effect of the thickness of perfluorinated ionomer-based interfacial layers on the performance of solution-processible phosphorescent devices was presented. Variation of the PFI thickness was

a major factor for the control of HOMO energy level of hole injection/transport layer stacks. Both for devices with vacuum-deposited and solution-processed electrophosphorescent emitters, insertion of relatively thin PFI layer between PEDOT:PSS and light emitting layer resulted in an improvement of current/power efficiency as well as lowering of driving voltage. "Efficiency behavior could be correlated with the shift of work function, which is induced by the change of surface chemical composition of PEDOT:PSS/PFI layers. Combinatorial design of hole/electron transport layer stacks, optimum emitter composition, and better electron injection/transport will provide more detailed understanding on the effects of ionomer-modified interfacial layers on the overall charge carrier balance and stability of soluble phosphorescent devices.

Acknowledgements

This research was supported by Basic Science Research Program through the National Research Foundation of Korea (NRF) funded by the Ministry of Education, Science and Technology (2009-0065638). This work was also supported by GRRC program of Gyeonggi province (GRRC Dankook 2011-B03; Development of nanostructured materials for next generation/flexible solar).

References

- [1] J.J. Park, S.T. Lee, T.J. Park, W.S. Jeon, J. Jang, J.H. Kwon, J. Kor. Phys. Soc. 55 (2009) 327.
- [2] M.-H. Kim, M.C. Suh, J.H. Kwon, B.D. Chin, Thin Solid Films 515 (2007) 4011.
- [3] T. Earmme, E. Ahmed, S.A. Jenekhe, Adv. Mater. 22 (2010) 4744.
- [4] P.K.H. Ho, J.S. Kim, J.H. Burroughes, H. Becker, S.F.Y. Li, T.M. Brown, F. Cacialli, R.H. Friend, Nature 404 (2000) 481.
- [5] P.K.H. Ho, M. Granström, R.H. Friend, N.C. Greenham, Adv. Mater. 10 (1998) 769.
- [6] J. Park, Y. Kwon, T.-W. Lee, Macromol. Rapid Commun. 28 (2007) 1366.
- [7] N. Rehmman, C. Ulbricht, A. Köhnen, P. Zacharias, M.C. Gather, D. Hertel, E. Holder, K. Meerholz, U.S. Schubert, Adv. Mater. 20 (2008) 129.
- [8] T.-W. Lee, Y. Chung, O. Kwon, J.-J. Park, Adv. Funct. Mater. 17 (2007) 390.
- [9] S.A. Choulis, V.-E. Choong, M.K. Mathai, F. So, Appl. Phys. Lett. 87 (2005) 113503.
- [10] X.H. Yang, F. Jaiser, B. Stiller, D. Neher, F. Galbrecht, U. Scherf, Adv. Funct. Mater. 16 (2006) 2156.
- [11] N.S. Kang, B.-K. Ju, J.W. Kim, J.-J. Kim, J.-W. Yu, B.D. Chin, J. Appl. Phys. 104 (2008) 024511.